Physical processes describing heat transfer at short lengthscale

Karl Joulain

PHYSICAL PROCESSES DESCRIBING HEAT TRANSFER AT SHORT LENGTHSCALE

Karl Joulain
ENSMA, Université de Poitiers, Laboratoire d'études thermiques, CNRS UMR 6608
B.P 40109, 86961 Futuroscope, France

Abstract

We explore in this article physical processes describing heat transfer at short time and length scales. First, we show that the physical phenomena describing classical heat transfer are no longer valid when the dimension involved goes below some characteristic lengths like the heat carrier mean free path or wavelength. In particular, we present heat transfer calculations in the ballistic regime when heat carriers fly from one border of the considered system to the other. Heat conduction which values in nature span only a range of 4 orders of magnitude will particularly focus our attention. We will show how the new development of nanotechnology paves the way to the conception of new very low thermal conductivity materials with outstandingly interesting properties. Finally, we will review thermal radiation properties in the near-field i.e. at subwavelength distances. We will see that at such distances, thermal radiation coherence properties drastically change and open the way to the conception of new thermal sources.

Introduction

Heat transfer can be defined as thermal energy in transit due to a spatial temperature difference (Incropera et al. 2006). Usually, three transfer modes are considered. Conduction, that refers to heat transfer across a material, convection occuring between a surface or a moving fluid and radiation describing the transfer in vacuum between different temperature bodies by means of electomagnetic waves. Classically, heat conduction is described by a diffusion equation. Radiative heat transfer is governed by the so called Radiative Transfer Equation (RTE). In convection, calculations are based on the existence of a boundary layer and the heat equation resolution in the layer.

At short scale, all these theories are invalidated when distances involved become smaller than characteristic lengths governing the phenomena physics. For example, in a fluid, when typical distances involved become smaller than particle mean free path, the concept of fluid cell is not pertinent anymore. In these conditions, hydrodynamics equations are not valid : particles in the fluid are flying from one side of the system to the other side. This phenomenon cannot be named convection anymore but molecular ballistic transfer. In the second section of this article, we will show through the example of transfer between two interfaces or between one tip and an interface how heat can be transmitted ballistically through air and reach a very high equivalent heat transfer coefficient.

The third section of this article will focus on heat conduction. In a solid, it is the principal heat transfer mode. Heat carriers can be free electrons of a metal or phonons in an insulator or a semiconductor. Like in gas, heat carriers in classical conditions are submitted to a lot of collisions. This leads to Fourier's law and to heat equation (Kim et al. 2007). When carriers mean free path is of the system size order, some carriers carry heat ballistically : heat transport is not a diffusion process. It resembles more to a ballistic process similar to that is occuring in thermal radiation. Heat flow obeys to the Boltzmann equation describing evolutions of a distribution function equivalent to a phonon or electron specific intensity. We will examine different collision processes occuring for phonons in solids. We will see through Boltzmann's

equation solution in different geometries such as film, wires or tube that it is possible to describe and predict thermal properties in nanostructures. We will note that concepts such as thermal conductivity have to be used very cautiously. When distances approach the electron or the phonon wavelength, quantum effects such as interference and quantification of the modes has to be taken into account (Chen 1999). We will see that in such nanoscale systems thermal conductance is quantified. (Schwab et al. 2000). Moreover, alternative stack of different material (superlattices) can form phononic crystals with forbidden frequency band gaps where phonons cannot propagate (Narayanamurti et al. 1979).

Radiative transfer will be treated in the fourth section. In participating medium, radiation is classically described by Radiative Transfer Equation and radiometry laws. When the system size is of the order of the thermal wavelength, wave effects appear. Thermal radiation has to be treated with fluctuational electrodynamics theory (Rytov et al. 1989). The principles of the calculation are the following : thermal motions initiates currents in materials that behave like an antenna and radiate an electromagnetic field. Interference and tunelling effects can then be dominant. Nevertheless, it can be shown that radiative heat transfer can be retrieved from the Maxwell equations and that specific intensity can be defined under certain conditions from the electromagnetic field.

At subwavelength distances, thermal emission is very different that in far field (Polder & Van Hove 1971, Joulain et al. 2005). For example, contrary to classical thermal radiation, thermal emission in near field i.e at subwavelength distances can be both spatially and temporally coherent, when additional modes such as surface polaritons or guided modes exist. Experiments have shown that these thermal emission near-field properties can be exploited to built thermal coherent sources by microstructuring surfaces supporting surface waves. (Greffet et al. 2002). Thermal emission in near field can also be a tool for new type of imagery or spectroscopy. Near field optical microscopy experiments (DeWilde et al. 2006) have shown that thermal emission can map the electromagnetic density of states near a surface or image subwavelength objects.

Heat transfer can also be reformulated : two bodies at different temperatures separated by a vacuum distance d still exchange heat. But, in fluctuational electrodynamics, heat flux given by the Poynting vector contains different contributions, electric, magnetic, propagative or evanescent. In accordance with the type of material involved, these different contributions can be dominant or negligible so that the transfer can occur for some specific electromagnetic polarization or frequency.

Heat transfer in a fluid

Classically, heat transfer in a fluid is based on Navier-Stokes and heat equation resolution. The assumption that the Knudsen number is small, that is the fluid is in the collision regime, is required to derive these equations. When the fluid is rarefied, the system obeys a more general equation called the Boltzmann equation (Reif 1965):

$$\frac{\partial f}{\partial t} + \mathbf{v}.\nabla_{\mathbf{r}} f + \mathbf{F}.\nabla_{\mathbf{v}} f = \left(\frac{\partial f}{\partial t}\right)_{\text{coll}} \tag{1}$$

where $f(\mathbf{r}, \mathbf{v}, t) d^3\mathbf{r} d^3\mathbf{v}$ is the average number of particles at a time t in an elementary volume $d^3\mathbf{r} d^3\mathbf{v}$ centered around $(\mathbf{r}, \mathbf{v})$. $\left(\frac{\partial f}{\partial t}\right)_{\text{coll}}$ is the collision contribution on the evolution of f. It is an integral over all the possible binary collisions that modifies f. Resolution of (1) is in general a difficult task. The Chapman Enskog development is the classical procedure to solve it (Balian 1996). At the first two orders of approximation, this development recovers Navier-Stokes and heat equation. At higher orders, other equations over macroscopic quantities can be found : the so-called Burnett and super-Burnett equations (Burnett 1936). Other resolution

procedures have been recently proposed (Struchtrup & Torrilhon 2003). Non trivial rarefied fluid behaviour can be predicted from these procedures. For example, a rarefied viscous fluid in a channel has its velocity field discontinuous at the wall.

Ballistic Transfer

An easy limit is the ballistic regime. It occurs in a fluid when the fluid particles undergo no collision along a path of the system size. Heat flux calculation in such a system is easy. Let us consider two planar interfaces at two different temperatures T_1 and T_2 and separated by a gap of width d filled with a gas. When the gas particle mean free path is much larger than the system size, the particles fly ballistically from one side of the system to the other one. We consider that the particles touching a surface at temperature T adopt instantaneously a Maxwellian velocity distribution function. Using the fact that the heat flux

$$\dot{\mathbf{q}} = \int \frac{1}{2} m v^2 \mathbf{v} f(\mathbf{v}) d^3\mathbf{v} \tag{2}$$

and that no particle flux exist between the interfaces ($\int \mathbf{v} f(\mathbf{v}) d^3\mathbf{v} = 0$) the heat flux reads (Carminati 2007)

$$\dot{\mathbf{q}}_{bal} = \frac{n\sqrt{T_1 T_2}(2k_B)^{3/2}}{\sqrt{\pi m}(\sqrt{T_1} + \sqrt{T_2})}(T_1 - T_2) \tag{3}$$

Let us note that the heat flux does not depend on the distance between interfaces. A heat transfer coefficient can also written when $T_1 \sim T_2 \sim T$:

$$h_{bal} = \frac{nT(2k_B)^{3/2}}{2\sqrt{\pi m T}} \tag{4}$$

At ambient temperature and for gaseous nitrogen, $h_{bal} = 1.310^5$ W m^{-2} K^{-1}. Note that the mean free path for nitrogen molecules in air is around 40 nm at ambient temperature. The diffusive regime is therefore valid until the distance is around 10 times the mean free path say 400nm. In this regime, air has roughly a thermal conductivity k of 0.024 W m^{-1} K^{-1}. For two interfaces separated by a 400 nm gap, a heat transfer coefficient $h = k/d = 6\ 10^4$ W m^{-2} K^{-1}.

We therefore see that ballistic heat transfer do exist when particles mean free path is smaller than the distance involved. Such a situation occur in near field microscopy between a tip and a substrate. Consider for example the typical case of a heated tip situated at a distance d of a substrate (Fig.1 left). This technology could be used for example in thermally assisted data storage. The principle is to heat a sample at a sufficient high temperature and at sufficiently high speed in order to write a bit on the sample (by vitreous transition or magnetic recording). The question to be solved is what is the heat flow deposited below the tip and at what scale? This problem can be addressed in the same way as the two interface situation in the ballistic regime. Nevertheless, the distance between the tip and the sample is often of the order of the molecules mean free path. In this mesoscopic regime, the effect of collision has to be taken into account. Chapuis et al. (Chapuis et al. 2006) have calculated the heat flux between a tip at 800 K and a sample at ambient temperature by means of a Monte Carlo method. Particles are emitted at the tip following a Maxwellian distribution. This particle may experienced a collision along a path of length L according to an exponential collision probability law $\exp(-l/L)$ where l is the mean free path. The results are presented in Fig.1 right. A very high heat flux density is reached. It has been shown also that powers of the order of 0.1 nW can be deposited for a few tens of ps allowing the possibility for thermally assisted storage.

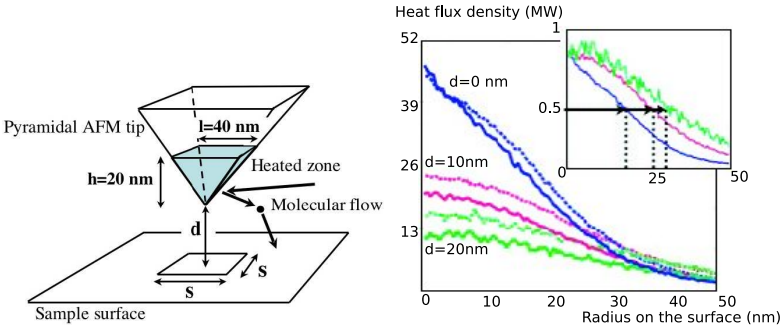

Figure 1: Left: Pyramidal AFM tip above a substrate. Typical length used are $l = 40$ nm and $h = 20$ nm. The distance d is in the nanometric range. Right: Heat flux density along the section of the sample for different tip-sample distances.

Conduction in solids

Thermal conduction in solids is also a phenomenon classically described by a diffusion process of heat carriers. An interesting feature to note about heat conduction in solids is that its magnitude does not change a lot with the materials concerned. For example, solids thermal conductivity spans only on four orders of magnitude contrary to electrical conductivity. Indeed, heat carriers can not only be electrons but also phonons in crystals. In metals, heat conduction due to electrons dominates over phonon conduction. In insulators, only phonon heat conduction is present, but it is impossible to be completely rid out of all heat carriers movement as it is the case for electrical conduction. Therefore, conduction due to the presence of acoustic waves in matter will always be present in the same way heat conduction is always present in gas due to the presence of molecules.

In a crystal, an analogy can be done with thermal radiation : instead of photons, heat is carried in solids by quasiparticles called phonons. These particles can be considered as boson in the same way photons are. At thermal equilibrium phonons are populated according to a distribution function that resembles to Planck's law. If the particles collides, the regime is diffusive and the heat flux follows the Fourier law (analogy with the Rosseland regime (Modest 2003)). When the phonons are not submitted to collisions, heat conduction behaves like radiation in a transparent medium.

Diffusive regime : Fourier's law and limits

Fourier's law is the fundamental macroscopic equation from which general equations such as the heat equation are derived.

$$\dot{\mathbf{q}}(\mathbf{r}, t) = -k\nabla T(\mathbf{r}, t) \tag{5}$$

The kinetic theory, which considers that heat carriers behave like a gas, is a way to establish the Fourier law. Let us come back to the Boltzmann equation reformulated for phonons or electrons. In the collision regime, the collision integral is often written in the so-called relaxation time approximation. In this model, it is stated that the main collison integral contribution is to relax the distribution function to a local equilibrium distribution function. In steady state, Boltzmann's equation reduces to

$$\mathbf{v}.\nabla_{\mathbf{r}} f = \frac{f^0 - f}{\tau(\mathbf{k})} \tag{6}$$

where $\mathbf{k}$ is the particle wavenumber, $f(\mathbf{r}, \mathbf{k}) d^3\mathbf{r} d^3\mathbf{k}$ is the number of phonons in the elementary volume $d^3\mathbf{r} d^3\mathbf{k}$. f^0 is thus a local equilibrium distribution function. For example, phonons in

a solid are in local thermal equilibrium when they follow the following function (Bose-Einstein distribution)

$$f^0(\mathbf{r},\mathbf{k}) = \frac{1}{\exp[\hbar\omega(\mathbf{k})/k_bT(\mathbf{r})]-1} \tag{7}$$

$\tau(\mathbf{k})$ is the phonon relaxation time or collision time. Different physical phenomena are at the origin of phonon collisions. The presence of impurities, stack defaults, dislocations or isotopes scatters phonons in the same way molecules or small particles of dust scatter phonon in the atmosphere (Klemens 1958, Holland 1964). Phonons can also be scattered at the system boundaries due to their roughness. Finally, the fact that crystal potential is not purely harmonic makes the phonons not to be system eigenmodes. They can be scattered through a non-linear process where one phonon can split into two phonons or, on the reverse process two phonons interact to give a single one. In this last process, when the resulting phonon lies in the so called Brillouin zone, this is a normal process (N). When, the resulting phonon is outside the zone, this is an Umklapp process (U). Due to crystal periodicity, the final phonon is in the opposite direction of the initial phonons. This last process is at the origin of thermal resistance (Landau & Lifshitz 1981).

Let us look for a solution of the form $f = f^0 + \eta f^0$ where $\eta \ll 1$. The Boltzmann equation (6) reads in presence of a temperature gradient $\eta f^0 = -\tau(\mathbf{k})\mathbf{v}.\nabla_\mathbf{r} T \partial f^0/\partial T$. Heat flux obtained from this Boltzmann equation solution is

$$\dot{\mathbf{q}}(\mathbf{r}) = -\sum_{\mathbf{k},p} \hbar\omega(\mathbf{k})\tau\mathbf{k}\frac{\partial f^0}{\partial T}(\mathbf{v}.\nabla T)\mathbf{v} = -\frac{1}{6\pi^2}\sum_p \int_0^{K_{Max}} C v_{k,p} v_{g,p}^2(k)\tau_p(k)dk \tag{8}$$

for an isotropic medium. In this last expression, the summation is done on the polarization p and wavevector k. $v_{g,p}$ is the group velocity of the polarization branch p, K_{Max} is the maximum phonon wave vector (Brillouin zone limit), C_v is the contribution to the thermal conductivity of one single mode $C_v = k_B x^2 e^x/(e^x-1)^2$ with $x = \hbar\omega/k_BT$.

Therefore, the thermal conductvity k depends on the temperature but also of the modes group velocities and relaxation times. The higher is velocity and the lower are the collisions, the larger is the thermal conductivity.

Low thermal conductivities

Low thermal conductivities would be very useful for thermal barrier or for thermoelectric materials. In the diffusive regime, the simplest way to decrease crystal thermal conductivity is to introduce impurities that scatters phonons. This is the so called alloy limit. It can be shown that phonon scattering cross section is very analogous to Rayleigh light scattering when the phonon wavelength is much larger than the scatterer : $\sigma \sim a^6/\lambda^4$ where a is the impurity typical size. The smaller is phonon wavelength, the more it is scattered. In alloys, the impurity size is of the order of 10^{-10}m. Impurities with larger sizes could scatter more efficiently phonon wavelength of the nanometer range that contribute the most to the thermal transport. This technique has been used (Kim et al. 2007, Chitirescu et al. 2007) where nanometer size particles are introduced in a bulk medium in order to reach thermal conductivity approaching those of strong insulators. In the same idea, materials with a large disorder like amorphous materials exhibit a low thermal conductivity, because the heat carriers mean free path is of a few atomic spacing. For examples, glasses like fused silica have a typical thermal conductivity of 1 W m^{-1} K^{-1}.

It is possible to decrease phonon mean free path increasing phonon collisions with borders. A way is to confine phonons in nanostructure such as nanofilms or nanowires. Thermal conductivity is then mostly governed by nanometric boundary conditions. In Fig. 2, we show nanowire

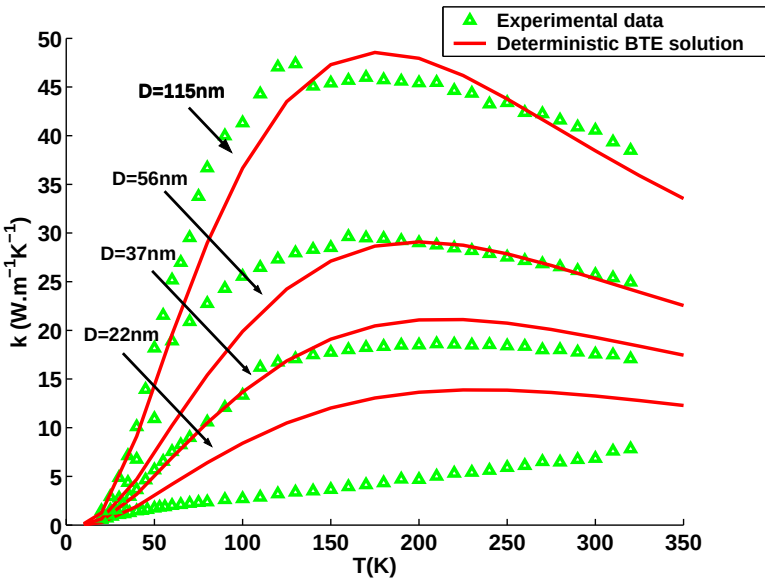

Figure 2: Silicon nanowire thermal conductivity for different wire diameter versus temperature. Calculations compared with experiments.

thermal conductvity calculation (Terris et al. 2007) compared with nanowire thermal conductivity measurements (Li et al. 2003). We see that Si nanowire thermal conductivity is highly reduced compared to bulk silicon. This is due to phonon scattering at wire boundaries. The same behaviour explains the in-plane conductivity decreasing in thin films, where the phonon mean-free path is of the order of the system width.

The other effect of phonon confinement is to modify phonon dispersion relation. The result is a reduction of phonon group velocity which has also a reduction effect on thermal conduction.

High thermal conductivities

High thermal conductivity materials are useful to design new heat sinks in electronics. Indeed, the increasing progress in nanotechnology has led to very high power dissipated in components. More efficient heat sinks are now required in order to ensure the electronic components thermal management. Following the reasoning done concerning low thermal conductivities, one can imagine two reasons for high conductivity. High phonon velocity and very long collision time. The phonon velocity, which can also be seen as a velocity of sound, is higher when molecular bound is stiff. For example, diamond is a well known thermal conductor with a thermal conductivity larger than 2300 W m^{-1} K^{-1}. Carbon nanotubes have been pointed to be very good thermal conductors from both theoretical calculations (Mingo & Broido 2005) and experiments (Kim et al. 2001, Fujii et al. 2005, Chang et al. 2006). Indeed, the stiffness of carbon atoms bounds is even higher than in diamond. Morevoer, carbon nanotube cylindrical structure makes that phonons follow their way along the surface of the nanotube without seeing any border. Thus, their collision time is very long. Single walled carbon nanotube seems to have particular high thermal conductivity whereas the results is more controversial concerning Multiwalled carbon nanotubes.

Ballistic regime

Fourier's law is valid when heat transport is in the diffusive regime. When it is not the case, i.e when heat carriers have a mean free path of the order of the typical system size, the transport

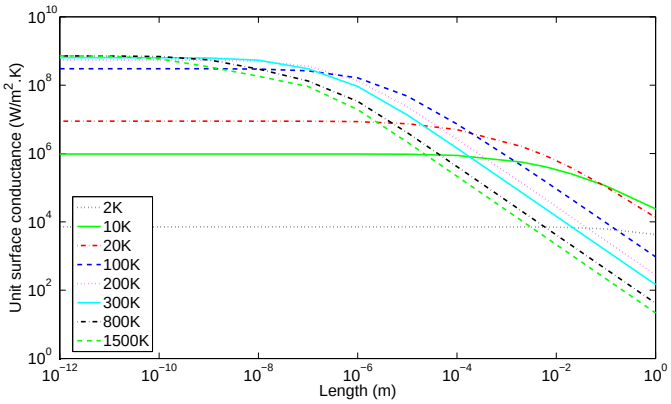

Figure 3: Surface thermal conductance of silicon films at different temperatures versus film thickness.

is mesoscopic or even ballistic when the mean free path is much lower than the system size. This last situation is particularly simple to analyse.

Let us consider as a simple illustration the following system : a solid which acoustic modes follow a single phonon branch in the Debye approximation (Kittel 2004) and with plane parallel borders (orthogonal to z direction) separated by a distance d are at temperatures T_1 and T_2 small compared to the Debye temperature. In this approximation, the specific phonon intensity emitted by a wall at temperature T reads :

$$I^0(\omega) = \frac{\hbar\omega^3}{2\pi^3 v_g^2[\exp(\hbar\omega/k_bT) - 1]} \tag{9}$$

Here the group velocity v_g is constant. The heat flux emitted by a wall at temperature T_1 is therefore :

$$q = \int_0^\infty d\omega \int_{\Omega=2\pi} I^0(\omega)\cos\theta d\Omega = \frac{k_b^4}{2\pi^2 v_g^2 \hbar^3}\int_0^\infty \frac{x^3 dx}{e^x - 1} T_1^4 = \sigma_{ph} T_1^4 \tag{10}$$

where θ is the angle between the direction z and the direction of the intensity considered, $\sigma_{ph} = k_b^4\pi^2/(30\hbar^3 v_g^2)$. The total heat flux exchanged is obtained by subtracting the heat flux emitted by the wall at temperature T_2 so that $\varphi = \sigma_{ph}(T_1^4 - T_2^4)$. We see that the heat flux does not depend on the distance between the two interfaces. Phonons are flying from one interface to the other. Conductive heat flux behaves like thermal radiation. If $T_1 \sim T_2 \sim T$, the total heat flux can be approximated by $\varphi \sim 4\sigma_{ph}T^3(T_1 - T_2)$. Following the definition of the thermal conductivity by the Fourier law, a ballistic conductivity along the z direction can be written :

$$k_z^{bal} = 4\sigma_{ph} d T^3 \tag{11}$$

This conductivity depends on the system size. This is the opposite situation from the bulk where thermal conductance depends on the system size and thermal conductivity is an intrisic material property. At small distance, thermal conductance is the relevant quantity independent on the system size, contrary to thermal conductivity.

Transition between diffusive and ballistic regime is exhibited in Fig.3 where surface thermal conductance in silicon films is represented versus film thickness in log-scale. At distances larger than 10 μm, conductance decreases as $1/d$ where d is the film thickness. The film behaves like the bulk. When the thickness is of the mean free path order, the film is in the mesoscopic regime. Film conductance still increases with decreasing thickness. At extremely

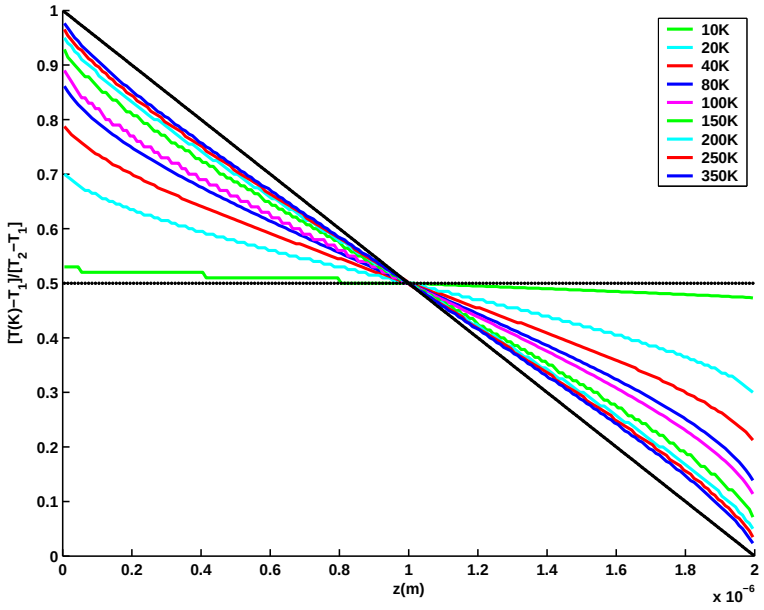

Figure 4: Temperature profile in a 2-micron-thick film for different temperatures. Note the transition between the Fourier regime (linear profile relating extreme temperatures) and the ballistic regime (flat profile).

small distance, the conductance is ballistic. Temperature inside the film confirms this behaviour (Fig.4). In the Fourier regime, the temperature profile is linear between extreme temperatures. In the mesoscopic regime, there exists a temperature jump at boundaries similar to temperature jumps occuring in thermal radiation for optically thin media. In the ballistic regime, the profile is flat. One therefore sees that thermal conductivity, which is undoubtetly linked to the Fourier law can hardly be used in the last two regimes.

Wave effects

Due to Bose-Einstein statistics, phonons in a material at temperature T are distributed according to a function that resembles the Planck law. Their wavelength are peaked around a value given by an analog of Wien's law. For example at ambient temperature, phonons wavelength peak around a few nanometer. When the temperature is in a few Kelvins order, the wavelength is a fraction of a micrometer. When the system characteristic size is of the order of phonon wavelength, wave effects appear. For example, phonons can tunnel across a junction such as a quantum well. In the case of superlattices, that are periodic stacks of alternating different materials, forbidden band gaps may open in phonon dispersion relation : propagation is not possible at band gap wavelengths. This phenomenon is analog to Bragg reflection in optics.

At low temperature, structures like nanowires can have their lateral size of the order of the most populated wire acoustic modes wavelength. At these wavelength, modes are quantified in the wire as optical modes are quantified in an optical fiber. Heat can only be carried at these special authorized modes. In a monodimensional structure, the heat flux between the system extremities separated by d at temperature T_1 and T_2 is :

$$\begin{aligned} \phi &= \frac{1}{L}\sum_{p,\mathbf{k}} \hbar\omega(\mathbf{k}) v_g(\mathbf{k}) \left[\frac{1}{\exp(\hbar\omega/kT_1)} - \frac{1}{\exp(\hbar\omega/kT_2)}\right] \\ &= \sum_p \int_0^{\omega_{max}} \frac{\hbar\omega d\omega}{\pi} \left[\frac{1}{\exp(\hbar\omega/kT_1)} - \frac{1}{\exp(\hbar\omega/kT_2)}\right] \end{aligned} \tag{12}$$

If $T_1 \sim T_2 \ll \omega_{max}$, the heat flux reads

$$\phi = \frac{\pi k^2}{6\hbar}\left(T_1^2 - T_2^2\right) \approx G_{quant}(T_1 - T_2) \tag{13}$$

where $G_{quant} = \pi k^2 T/3\hbar$ is the quantum of conductance. Such a quantum of conductance has been observed by Roukes et al.(Schwab et al. 2000) at low temperature for suspended wire.

Radiative heat transfer

Classical heat transfer is based on the concepts of radiometry i.e. of geometrical optics. Ray lights propagate in straight line and wave effects such as interferences and tunelling are not taken into account. This approximation fails when distances involved go below the typical wavelength. As in the case of light propagation, phenomena such as diffraction occur when light is confined at a subwavelength size. Fluctuational electrodynamics is the theory which has to be used to treat such problems.

Fluctuational electrodynamics

The framework of fluctuational electrodynamics has been introduced by Rytov (Rytov et al. 1989). The idea is that in any material at thermal equilibrium, random thermal fluctuations make charges such as electrons or ions moving. These charge motions initiate thermal currents that radiate an electromagnetic field. From an electromagnetic point of view, the problem will be solved if the currents characteristics are known as well as the radiation of an elementary dipole in the geometry considered. The currents are actually given through their cross-spectral correlation function by the fluctuation-dissipation theorem (FDT) whereas the system Green function gives the answer to the radiation problem.

In a medium at thermal equilibrium T characterized by its dielectric constant ϵ, thermal electric currents cross spectral correlation function is given by the FDT

$$\langle j_k(\mathbf{r},\omega) j_l(\mathbf{r}',\omega')\rangle = 4\pi\epsilon_0 Im(\epsilon)\Theta(\omega,T)\delta_{kl}\delta(\mathbf{r}-\mathbf{r}')\delta(\omega-\omega') \tag{14}$$

where Θ is the mean energy of an oscillator $\Theta(\omega,T) = \hbar\omega/[\exp(\hbar\omega/k_bT) - 1]$. The electromagnetic field is related to the currents by the system Green function. For example, the electric field reads

$$\mathbf{E}(\mathbf{r},\omega) = i\mu_0\omega \int \overleftrightarrow{\mathbf{G}}(\mathbf{r},\mathbf{r}',\omega).\mathbf{j}(\mathbf{r}',\omega)d^3\mathbf{r}' \tag{15}$$

In thermal radiation, we are interested in quantities such as the emitted radiative flux given by the Poynting vector $1/2Re\left[\langle \mathbf{E}(\mathbf{r},\omega) \times \mathbf{H}^*(\mathbf{r},\omega))\rangle\right]$ and the density of energy. It can be shown that the specific intensity itself is related to a Wigner transform of the electric field cross spectral correlation function (Apresyan & Kravtsov 1996). Therefore, we have to calculate quantities such as $\langle \mathbf{E}(\mathbf{r},\omega)\mathbf{E}^*(\mathbf{r}',\omega)\rangle$. In all these equations, the brakets denote ensemble average over all the system realization.

Thermal radiation near an interface

The Green function of a system consisting of an interface separating a dielectric (medium 2) from a vacuum (medium 1) is well known. It is then straightforward to apply the FDT to currents in the heat flux or energy density expressions. The result is an integration over the wavevector parallel to the interface K and represents the summation of the individual plane wave contributions. The heat flux reads

$$\langle S_z(\mathbf{r},\omega)\rangle = \frac{\hbar\omega}{4\pi^2}\frac{1}{e^{\hbar\omega/(k_bT)} - 1}\int_0^{\omega/c} KdK\left(1 - |r_{12}^s|^2 + 1 - |r_{12}^p|^2\right) \tag{16}$$

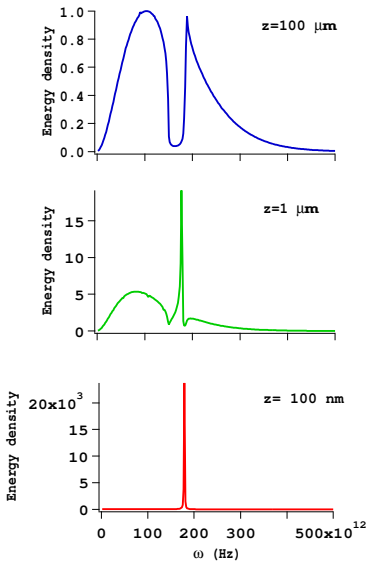

Figure 5: Energy density above a semi-infinite medium of SiC at $T = 300$ K.

whereas the energy density expression reads

$$u(\omega,T) = \frac{\Theta(\omega,T)\omega}{2\pi^2c^2}\int_0^{\omega/c}\frac{KdK}{\gamma_1}\left(\frac{1-|r_{12}^s|^2}{2}+\frac{1-|r_{12}^p|^2}{2}\right) + \frac{\Theta(\omega,T)\omega}{2\pi^2c^2}\int_{\omega/c}^{\infty}\frac{K^3dK}{k_0^2|\gamma_1|}\left[Im(r_{12}^s)+Im(r_{12}^p)\right]e^{-2|\gamma_1|z} \quad (17)$$

In the preceding expressions, r_{12}^{λ} is the Fresnel reflection coefficient in $\lambda = s, p$ polarization. γ_1 is the wavevector component perpendicular to the interface.

The heat flux expression is similar to the classical one. Only propagative waves are emitted and carry energy from a heated body. Emissivity can be identified from the heat flux expression. It is equal to $1/2(1-|r_{12}^s|^2+1-|r_{12}^p|^2)$.

Energy density has not only a propagative contribution, but also a contribution from the evanescent waves. Due to the exponentially decaying term, this contribution only exists if the distance to the interface is smaller than the wavelength considered. This supplementary term depends on the imaginary part of the surface reflection coefficient. A blackbody, for example, has no envanescent wave contribution to the energy density near its surface. If the reflection coefficient imaginary part is large, the difference in the energy density near or far from the surface is very important. This occurs in particular close to materials that exhibit surface waves such as polar materials (SiC or Silica). Surface waves are evanescent waves that propagate along the interface but decay exponentially in both directions perpendicular to the interface. They are associated to polarization waves in the material such as plasmon of phonon-polaritons (Ashcroft & Mermin 1976). In Fig.5 from (Shchegrov et al. 2000), energy density spectrum above a semi infinite medium of SiC separated from vacuum by an interface is represented. We note that at distances large compared to the mean wavelength, the energy spectrum is very similar to a blackbody spectrum. When the distance to the interface is reduced, the energy density increases at a particular frequency. At a 100nm distance, the energy density spectrum is almost monochromatic. In the case of SiC, this peak is due to the presence of surface waves (phonon polaritons). At the peak frequency, the density of electromagnetic modes increases due to the presence of phonon polaritons.

At thermal equilibrium, energy density reads as the product of the electromagnetic density of states by the mean energy of an oscillator. Therefore, an instrument able to measure the

electromagnetic energy density close to a surface also measures the electromagnetic density of states (Joulain et al. 2003). This instrument exists. This is an apertureless Scanning Near-Field Optical Microscope. An AFM tip approached at a nanometric distance of an interface can scatter the evanescent thermal field and convert evanescent waves into propagating waves that can be detected by a classical optical device. This experiment has been performed by De Wilde et al. (DeWilde et al. 2006). Note that this kind of instrument is nothing else than an infrared near-field microscope where illuminated light is thermal radiation emitted by the sample.

Near-field thermal exchange between two semi-infinte bodies

Let us consider two flat interfaces delimiting two semi-infinite bodies separated by a distance d in vacuum. The two bodies are maintained at their temperature T_1 and T_2 and a heat flux is exchanged between the two bodies. This heat flux is obtained through the calculation of the Poynting vector ensemble average by means of the fluctuation dissipation theorem. As in the single plane interface case, the heat flux expresses as a summation of the individual plane waves. Two contributions can be identified:

$$\begin{aligned} q^{prop}(\omega) &= \sum_{i=s,p} \int \frac{d\omega d\Omega \cos\theta}{2} \left[\frac{(1-|r_{31}^i|^2)(1-|r_{31}^i|^2)}{|1-r_{31}^i r_{32}^i e^{2i\gamma_3 d}|^2} \right] \left[L_\omega^0(T_1) - L_\omega^0(T_2) \right] \\ q^{evan}(\omega) &= \sum_{i=s,p} \int d\omega \int_{\omega/c}^{\infty} 2K dK e^{-2Im(\gamma_3)d} \left[\frac{Im(r_{31}^i) Im(r_{32}^i)}{|1-r_{31}^i r_{32}^i e^{2i\gamma_3 d}|^2} \right] \frac{[L_\omega^0(T_1) - L_\omega^0(T_2)]}{k_0^2} \end{aligned} \quad (18)$$

where L_ω^0 is the blackbody specific intensity. q^{prop} denotes the propagative wave contribution. It is very close to the classical expression provided that the emissivity is identified to $1-|r_{12}|^2$. Nevertheless, the denominator, a Fabry-Perot like expression with a rapidly fluctuating term is slightly different from the classical expression. After summation on the angular frequency, it can be averaged so that the propagative contribution can be indentified to

$$q^{class}(\omega) = \sum_{i=s,p} \int \frac{d\omega d\Omega \cos\theta}{2} \left[\frac{\epsilon_1' \epsilon_2'}{1-\rho_1\rho_2} \right] \left[L_\omega^0(T_1) - L_\omega^0(T_2) \right] \quad (19)$$

which is the classical radiative heat transfer flux between two opaque blackbodies. Here, ϵ' and ρ are the material emissivity and reflectivity. The evanescent contribution describes the heat flux due to tunnelling. This term is important when the reflection coefficient imaginary part is important. This can happen for material supporting surface waves when the surface waves supported by each of the interfaces interact each other. In Fig.6(a), the heat transfer coefficient ($h^R(\omega) = \lim_{T_1-T_2} q(\omega)/(T_1-T_2)$) is represented for SiC and glass versus sample separation distances. We note that $h^R(\omega)$ increases as $1/d^2$ at small distances. We also note in Fig.6(b) that the heat transfer coefficient is almost monochromatic important at the resonant surface wave frequency, where the collision between the polaritons occurs. This collision process between polaritons also exists in bulk materials and is responsible of thermal conduction due to optical phonon modes (Joulain 2007)

The heat transfer also increases when two metals are approched to each other but for completely different reasons : eddy currents appear at the surface metal creating an important magnetic near-field (Chapuis et al. 2008)

Radiation spatial coherence properties

Spatial coherence of a field is related to its cross spectral correlation function. The field is spatially coherent on a distance r if its component can interfere when taken at two different

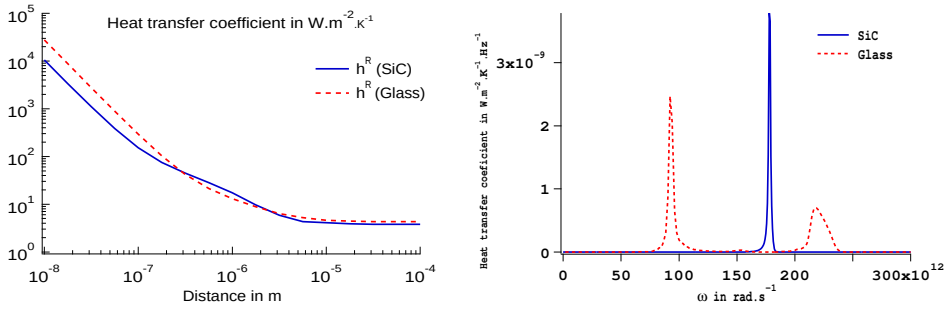

Figure 6: (a) Heat transfer coefficient for two semi-infinite samples of SiC or glass at $T = 300$ K versus separation distance d. (b) Monochromatic heat transfer coefficient for two semi-infinite samples of SiC or glass at $T = 300$ K for $d = 10$ nm.

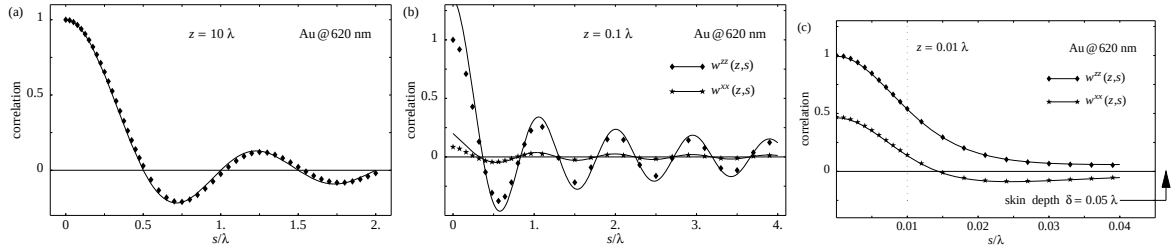

Figure 7: Electric field correlation function versus separation distance normalized to the wavelength. The different curves represents the field correlation above gold at 620 nm. (a) Correlation in far field : the correlation length is about $\lambda/2$. (b) Correlation in the surface wave regime : the correlation length is a few tens of the gold surface plasmon wavelength. (c) Correlation in the extreme near field : the correlation length is of the order of the distance to the interface.

points separated by r. Electromagnetic field cross spectral correlation function can be obtained by the FDT. Thermal radiation field emitted by a blackbody is correlated on a maximum distance of the order $\lambda/2$. In the near-field, the electromagnetic field correlation length is radically changed depending on the nature of the thermal evanescent electromagnetic field (Fig.7). At a surface plasmon wavelength, the electromagnetic field correlation function is determined by the surface wave propagation distance along the interface. In the extreme near-field, the field is static. Retardation effects disappear and the field is correlated on the order of the distance to the interface. Therefore, thermal electromagnetic field coherence greatly changes depending on the regime considered.

These near-field correlation properties have been exploited to design and construct thermal sources that are spatially coherent (i.e are directional) in the far-field. The idea is to rule a grating on a material that support surface waves in a wavelength domain where thermal emission is important. The physical process is the following. Thermally excited surface waves propagate along the interface and are scattered by the grating lines that are regularly spaced. In the far field, and for a particular direction, scattered waves interfere constructively. This kind of grating has been succesfully ruled on SiC to give a spatially coherent thermal source (Greffet et al. 2002). The source emission diagram is represented in Fig.8. Coherent thermal sources based on a waveguide rather than a material supporting surface waves have been designed. Guided waves propagate along the guide on which a grating has been ruled. Scattered guided waves interfere in the far-field to produce emission in a particular direction (Joulain & Loizeau 2007).

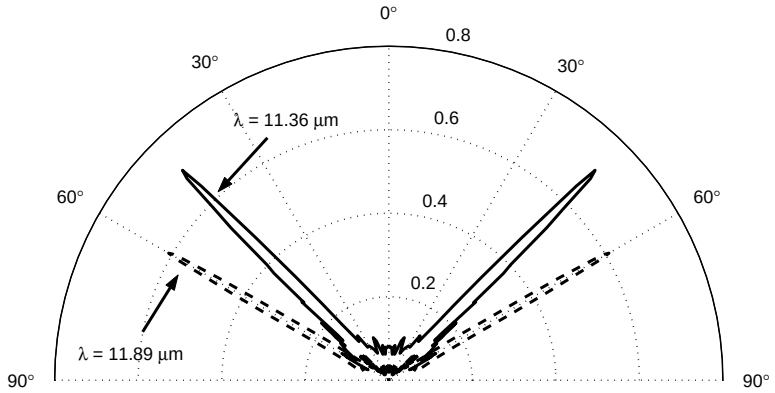

Figure 8: SiC grating emission diragram at two different wavelengths. Grating period : $\Lambda = 6.25$ μm, filling factor $F = 0.5$ and height $h = 0.285$ μm.

Conclusion

We have investigated in this paper physical phenomena that underlie heat transfer at microscopic scale. We have seen that depending on the distances involved, the phyics explaining heat transfer is not the same. Two typical lengths are determinant. Mean free path and wavelength heat carriers. When the carriers mean free path is small compared to the system size, the system is diffusive and obeys a diffusion equation like the heat equation. In the opposite situation, the transfer is ballistic and does not depend on the system size. At distances large compared to the carriers wavelength, wave effects are not present. Carriers behave like particles going in straight line and obey Boltzmann equation. At subwavelength distances on the contrary, band gaps open and transfer is forbidden at some frequency. Phonon filtering is then possible in order to reduce thermal transfer. The increasing improvement in nanotechnology has open the way to reach and go below these two characteristic lengths. It is now possible to engineer nanocomponent thermal properties in order to create new materials with exciting properties such as thermal barriers, heat sink or very high efficiency thermoelectric converters.

References

Apresyan, L. & Kravtsov, Y. A. (1996), *Radiation Transfer. Statisitical and wave aspects.*, Gordon and Breach, Amsterdam.

Ashcroft, N. & Mermin, N. (1976), *Solid state physics*, international edn, Saunders College, Philiadelphia.

Balian, R. (1996), 'De la mécanique statistique hors équilibre aux équations de transport', *Ann. Phys. Fr* **21**, 437.

Burnett, D. (1936), *Proc. Math. Soc. (London)* **40**, 382.

Carminati, R. (2007), *Microscale and nanoscale heat transfer*, Springer, chapter 2.

Chang, C. W., Fennimore, A. M., Afanasiev, A., Okawa, D., Ikuno, T., Garcia, H., Li, D., Majumdar, A. & Zettl, A. (2006), 'Isotope effect on the thermal conductivity of boron nitride nanotubes', *Physical Review Letters* **97**(8), 085901.

Chapuis, P., Greffet, J.-J., Joulain, K. & Volz, S. (2006), *Nanotechnology* **17**, 2978–2981.

Chapuis, P., Volz, S., Henkel, C., Joulain, K. & Greffet, J.-J. (2008), *Phys. Rev. B* **77**, 035431.

Chen, G. (1999), 'Phonon wave heat conduction in thin films and superlattices', *ASME J. Heat Transfer* **121**, 945–953.

Chitirescu, C., Cahill, D., Nguyen, N., Johnson, D., Bodapati, A., Keblinski, P. & Zschack, P. (2007), 'Ultra-low thermal conductivity in disordered, layered crystals', *Science* **315**, 351.

DeWilde, Y., Formanek, F., Carminati, R., Gralak, B., Lemoine, P., Joulain, K., Mulet, J.-P., Chen, Y. & Greffet, J. (2006), 'Thermal radiation scanning tunnelling microscopy', *Nature* **444**, 740–743.

Fujii, M., Zhang, X., Xie, H., Ago, H., Takahashi, K., Ikuta, T., Abe, H. & Shimizu, T. (2005), 'Measuring the thermal conductivity of a single carbon nanotube', *Physical Review Letters* **95**(6), 065502.

Greffet, J.-J., Carminati, R., Joulain, K., Mulet, J.-P., Mainguy, S. & Chen, Y. (2002), 'Coherent emission of light by thermal sources', *Nature* **416**, 61.

Holland, M. (1964), 'Phonon scattering in semiconductors from thermal conductivity studies', *Phys. Rev.* **134**(2A), A471–A480.

Incropera, F., Dewitt, D. & Bergman, T. (2006), *Fundamentals of heat and mass transfer*, 6^{th} edn, John Wiley and Sons, New-York.

Joulain, K. (2007), *J. Quant. Spec. Rad. Transf.* **109**, 294–304.

Joulain, K., Carminati, R. & J.-P. Mulet, J.-J. G. (2003), 'Definition and measurement of the local density of electromagnetic states close to an interface', *Phys. Rev. B* **68**, 245405.

Joulain, K. & Loizeau, A. (2007), *J. Quant. Spec. Rad. Transf.* **104**, 208–216.

Joulain, K., Mulet, J.-P., Marquier, F., Carminati, R. & Greffet, J.-J. (2005), 'Surface electromagnetic waves thermally excited : Radiative heat transfer, coherence properties and casimir forces revisited in the near field', *Surf. Sci. Rep* **57**(3-4), 59–112.

Kim, P., Shi, L., Majumdar, A. & Euen, P. M. (2001), *Phys. Rev. Lett.* **87**, 215502.

Kim, W., Wang, R. & Majumdar, A. (2007), 'Nanostructuring expands thermal limits', *Nanotoday* **2**, 40–47.

Kittel, C. (2004), *Introduction to solid state physics*, 8 edn, John Wiley ans sons, Philiadelphia.

Klemens, P. (1958), *Solid State Physics*, Vol. 7, Academic Press Inc., New York.

Landau, L. & Lifshitz, E. (1981), *Physical kinetics : volume 10 (Course of theoretical physics)*, Pergamon Press, Oxford.

Li, D., Wu, Y., Kim, P., Yang, P. & Majumdar, A. (2003), *Appl. Phys. Lett.* **83**, 2934–2936.

Mingo, N. & Broido, D. (2005), *Phys. Rev. Lett.* **95**, 096105.

Modest, M. (2003), *Radiative Heat Transfer*, second edn, Academic Press, San Diego.

Narayanamurti, V., Störmer, H. L., Chin, M. A., Gossard, A. C. & Wiegmann, W. (1979), 'Selective transmission of high-frequency phonons by a superlattice: The "dielectric" phonon filter', *Phys. Rev. Lett.* **43**(27), 2012–2016.

Polder, D. & Van Hove, M. (1971), 'Theory of radiative heat transfer between closely spaced bodies', *Phys. Rev. B* **4**(10), 3303–3314.

Reif, F. (1965), *Statistical and thermal physics*, McGraw-Hill, New-York.

Rytov, S., Kravtsov, Y. & Tatarskii, V. (1989), *Principles of Statistical Radiophysics*, Vol. 3, Springer-Verlag, Berlin.

Schwab, K., Henriksen, E., Worlock, J. & Roukes, M. (2000), 'Measurement of the quantum of thermal conductance', *Nature (London)* **404**, 974–976.

Shchegrov, A., Joulain, K., Carminati, R. & Greffet, J.-J. (2000), *Phys. Rev. Lett.* **85**, 1548.

Struchtrup, H. & Torrilhon, M. (2003), *Phys. Fluids* **15**, 2268–2280.

Terris, D., Joulain, K., Lacroix, D. & Lemonnier, D. (2007), 'Numerical simulation of transient phonon heat transfer in silicon nanowires and nanofilms', *Journal of Physics: Conference Series* **92**, 012077.